Modelling and simulation of the mechanical response of a Dacron graft in the pressurization test and an end-to-end anastomosis

Article *in* Journal of the Mechanical Behavior of Biomedical Materials · January 2016

DOI: 10.1016/j.jmbbm.2016.01.005

3 authors:

Claudio A. Bustos
University of Santiago, Chile

Claudio M Garcia-Herrera
University of Santiago, Chile

Diego J. Celentano
Pontificia Universidad Católica de Chile

Modelling and simulation of the mechanical response of a Dacron graft in the pressurization test and an end–to–end anastomosis

Claudio A. Bustos[a], Claudio M. García–Herrera[a]*, Diego J. Celentano[b]

a: Departamento de Ingeniería Mecánica, Universidad de Santiago de Chile, USACH, Av. Bernardo O'Higgins 3363, Santiago de Chile, Chile
b: Departamento de Ingeniería Mecánica y Metalúrgica, Pontificia Universidad Católica de Chile, Av. Vicuña Mackenna 4860, Santiago de Chile, Chile

Abstract

This work presents the modeling and simulation of the mechanical response of a Dacron graft in the pressurization test and its clinical application in the analysis of an end-to-end anastomosis. Both problems are studied via an anisotropic constitutive model that was calibrated by means of previously reported uniaxial tensile tests. First, the simulation of the pressurization test allows the validation of the experimental material characterization that included tests carried out for different levels of axial stretching. Then, the analysis of an end–to–end anastomosis under an idealized geometry is proposed. This case consists in evaluating the mechanical performance of the graft together with the stresses and deformations in the neighborhood of the Dacron with the artery. This research contributes important data to understand the functioning of the graft and the possibility of extending the analysis to complex numerical cases like its insertion in the aortic arch.

Keywords: Dacron; Mechanical characterisation; Modelling; Finite elements

1 INTRODUCTION

Aortic diseases can be derived from connective tissue disorders of the arterial wall and may consequenly lead to the formation of aneurysms. The compromised arterial tissue needs to be replaced using a Dacron prosthesis as a substitute (De Paulis et al., 2007). For the ascending aorta region, in particular, the continuous cardiac motion deteriorates the aneurysm wall and may lead to the rupture or complete dissection of the aorta, with a mortality rate of 94% (Johansson et al., 1995).

There are two surgical techniques for the insertion of the Dacron, the so-called Bentall-DeBono and David, such that their use depends on the degree of damage of the dilated tissue.

*Corresponding author: `claudio.garcia@usach.cl`

In these techniques, the patients are subjected to an induced cardiac arrest (cold cardioplegia) that adds a high degree of risk. Then, the damaged tissue is replaced by the graft constituting the end-to-end anastomosis between the proximal and distal zones, suturing continuously and adding a surgical adhesive reinforcement based on cyanocrylate (Doty et al., 2012).

Due to its good postoperative performance, Dacron has been used because of its ease of insertion, great resistance, dimensional stability, and good compatibility with the medium. The prosthesis consists of a corrugated tubular structure that provides axial flexibility to facilitate rapid implantation. The material is made of a woven of PET (polyethylene terephthalate) fibers arranged orthogonally. However, due to its composition, there can be instrinsic faults after seven years, with an incidence of 0.5 to 3% (Berger et al., 1981). Various studies have pointed out that the rigidity introduced by the insertion of the Dacron modifies the hemodynamics and the systolic pulse, causing greater shear stress and turbulence in the distal anastomosis (Chandran et al., 1992; Vardoulis et al., 2011). These effects can aggravate vascular diseases, affecting the function of the aortic valve and, near the anastomosis, the appearance of hyperplasia, damaging the endothelium and reducing the permeability of the graft with the possibility of pseudoaneurysms (Van Damme et al., 2005; Tremblay et al., 2009). These drawbacks set up important challenges to be able to predict realistically the mechanical response of the prosthesis under physiological pressurization states.

Regarding to the mechanical characterization of Dacron, few papers have been reported to date. Those by Hasegawa et al. (1979), Lee et al. (1986), Tremblay et al. (2009) only described and analyzed the experimental response, showing by means of tensile tests its marked anisotropy and influence of the corrugation. On the other hand, the work by Tai et al. (2000) evaluated the performance of a knotted graft in the pressurization test under physiological conditions. The results showed a practically constant response for the relative variation of the diameter with respect to the arterial pressure (compliance), putting in evidence the little capacity of the graft to damp the pulsating wave.

The objective of the present work consists in modeling the anisotropic mechanical response of a Dacron graft in the pressurization test and its clinical application in the simulation of an end-to-end anastomosis. For this purpose, a hyperelastic model, whose material parameters were obtained by means of previously reported uniaxial tensile tests, is used to simulate the pressurization test and compare this prediction with the experimental results obtained for different levels of axial stretching. This model is then applied to an end-to-end anastomosis to determine the stress condition that is generated based on an idealized geometry under normotensive and hypertensive conditions. The materials and methods used are described in Section 2: the experimental procedure in Section 2.1 and the constitutive modelling in Section 2.2. The experimental and numerical results are shown in Section 3 and discussed in Section 4. In particular, the results of the simulation of the pressurization test presented in Section 3.1 clearly demonstrate the validity of the constitutive model used. Moreover, the numerical predictions for the analyzed anastomosis shown in Section 3.2 put in evidence the complex stress scenario that are developed in terms of the adopted aorta properties.

2 MATERIALS AND METHODS

2.1 EXPERIMENTAL PROCEDURE

2.1.1 MATERIAL

The material used for all the tests was a Boston Scientific *Hemashield Platinum woven* Dacron prosthesis. It has a straight corrugated tubular configuration covered with a double layer impregnated with bovine collagen; see Figure 1.

The prosthesis has a nominal inner diameter of 24 mm and a length of 215 mm considering the corrugation folding. Specimens for the pressurization tests were obtained from it. Figure 2 shows the configuration of the corrugation folds, which were obtained digitally under an optical microscope.

2.1.2 PRESSURIZATION TEST

The pressurization test consists of a biaxial structural test that attempts to represent the *in-vivo* working conditions of the graft. Here, a Dacron segment is subjected to a constant axial stretching, evaluating the behavior of the diameter as pressure is injected into it. Generally, the response is obtained under different axial stretchings in order to avoid buckling due to the tube lateral flexibility.

Figure 3 shows the experimental setup used in this work, which is described in Guinea et al. (2005). Each test is carried out immersed in normal saline solution at 37 ± 1^{o}C. A *Keyence* optical extensometer (± 50 μm precision) was used to measure the outer diameter. The tested segments had an effective length of 64 mm between the inlet and outlet nozzles that were attached by means of worm drive hose clamps. A 33 mm diameter latex membrane was also added to prevent transmural leakage during the pressurization due to the material porosity. This diameter was adequate to avoid altering the response of the material, since the circumferential deformation did not exceed 3%.

Each segment was tested for two longitudinal stretchings λ_z of 1.25 and 1.30, such that $\lambda_z = l/l_0$, where l corresponds to the current length and l0 to the initial length. The samples were previosuly subjected to two stretching cycles up to $\lambda_z = 1.1$, with an una extension rate of 0.3 mm/s, in order to allow the corrugation be unfolded uniformly. After pulling the sample until the above defined longitudinal stretchings, the inner pressure was then applied, at a mean flow rate of 150 mL/min of warm normal saline, by making 20 loading–unloading cycles where the first 5 corresponded to conditioning cyles. The pressure was kept within the range of physiological interest (from 0 to 240 mmHg). The pressure and the outer diameter were recorded at all times.

The experimental results yield the inner pressure P_i curves as a function of the circumferential stretching λ_θ for the analyzed longitudinal λ_z stretching levels. The circumferential stretching is defined as $\lambda_\theta = d/d_0$, where d is the instantaneous diameter while the inner pressure is applied and d_0 is the outer diameter when there is no longitudinal stretching and the applied pressure is zero.

2.2 CONSTITUTIVE MODELLING

The constitutive model for the Dacron graft analyzed in this work is an extension of that proposed by Planas et al. (2007), which considers a deformable matrix reinforced by a dispersion of fibres. This model proposes a macroscopic approximation equivalent to the microscopic description of the reinforcing fibres, obtained by equating the mechanical deformation power of the fibres with the power of the effective continuum mediuum per unit volume in the reference configuration. Thus, the Second *Piola-Kirchhoff* stress tensor of the fibres $\boldsymbol{S}_{fibres}$ is:

$$\boldsymbol{S}_{fibres} = \sum_{\Theta=1}^{m} \frac{{f_f}^{\Theta} {s_f}^{\Theta}}{\lambda_f^{\Theta}} \left(\boldsymbol{N}_{\Theta} \otimes \boldsymbol{N}_{\Theta}\right) \tag{1}$$

where f_f^{Θ} is the volume fraction of the different m families of the fibres Θ, so that $\sum_{\Theta=1}^{m} f_f^{\Theta} = 1$, $\mathbf{N_{\Theta}}$ is the direction of the family of fibres Θ and s_f^{Θ} is the nominal stress that relates the mechanical behaviour of the fibres Θ with the respective stretching $\lambda_f^{\Theta} = \sqrt{\boldsymbol{C}\boldsymbol{N}_{\Theta} \cdot \boldsymbol{N}_{\Theta}}$. In addition, $\boldsymbol{C} = \boldsymbol{F}^T\boldsymbol{F}$ is the *Cauchy-Green* tensor, where $\boldsymbol{F}$ is the deformation gradient tensor with $J = det\boldsymbol{F}$.

The Second *Piola-Kirchhoff* stress tensor of the composite material (fibres + matrix) under the incompressibility hypothesis ($J = 1$) is:

$$\boldsymbol{S} = \boldsymbol{S}_{fibres} + 2\frac{\partial W_{matrix}}{\partial \boldsymbol{C}} \tag{2}$$

where W_{matrix} is the strain energy function of the hyperelastic material of the matrix.

The constitutive elastic tensor that can be derived from equation 2 is:

$$\mathbb{C} = \sum_{\Theta=1}^{m} \frac{f_f^{\Theta}}{\lambda_f^{\Theta 2}} \left[\frac{\partial s_f^{\Theta}}{\partial \lambda_f^{\Theta}} - s_f^{\Theta}\frac{1}{\lambda_f^{\Theta}}\right] \left(\boldsymbol{N}_{\Theta} \otimes \boldsymbol{N}_{\Theta} \otimes \boldsymbol{N}_{\Theta} \otimes \boldsymbol{N}_{\Theta}\right) + 4\frac{\partial^2 W_{matrix}}{\partial \boldsymbol{C} \otimes \partial \boldsymbol{C}} \tag{3}$$

In this work, the following definitions are adopted:

$$s_f^{\Theta} = s_f^{\Theta}(\lambda_f^{\Theta}) = \sum_{i=1}^{3} K_i(\lambda_f^{\Theta} - 1)^i \tag{4}$$

$$W_{matrix} = \mu(I_1 - 3)/2 \tag{5}$$

where K_i are positive material parameters of the fibres, μ is the a material parameter of the matrix and I_1 is the first invariant of the *Cauchy-Green* tensor $\boldsymbol{C}$.

This model has been firstly calibrated for the Dacron graft by using an experimental-numerical methodology applied to uniaxial tensile tests and, afterwards, validated by means of the simulation of the myograph tensile test. The parameters derived from this fitting are shown in Table 1 (note that $m = 2$, where superindexes *circ* and *long* respectively refer to circumferential and longitudinal fibres). The details of the characterization of the material are described in Bustos et al. (2015).

In relation to the simulation of the end–to–end anastomosis, a hyperelastic isotropic model has been considered to describe the mechanical response of the aorta segment (García–Herrera and Celentano, 2013; García–Herrera et al., 2013). In particular, the energy function proposed by Demiray (1972) was found to reasonably predict the response at high deformation levels. It is expressed as:

$$W = \frac{a}{b}\left[\exp\left(\frac{b}{2}(I_1 - 3)\right)\right] \tag{6}$$

where a and b are the positive constants of the material, with parameter a representing the initial slope of the Cauchy stress versus stretching curve in the simple tensile test.

Specifically, the parameters used for the analyzed cases are adjusted from donor patients aged 16–36 years (young) and 38–62 years (adults) according to the work by García-Herrera and Celentano (2013). Table 2 shows the determined parameters together with the rupture limits in the circumferential direction for the tensile test.

These constitutive models were implemented in an in-house finite element code extensively validated in many biomechanical applications (García–Herrera et al., 2012, 2013).

2.3 NUMERICAL SIMULATIONS

2.3.1 PRESSURIZATION TEST

The geometry analyzed for the simulation of the pressurization test consists of a 4.5^o 3D sector considering half the Dacron tube with an inner diameter of 24 mm and a length of 32 mm; see Figure 4. The boundary conditions were as follows. The vertical displacement in the middle region of the sample (symmetry condition) was restricted. The simulation considered two stages: 1) A displacement v is applied to the prosthesis to achieve the axial stretching, and 2) an inner pressure P_i is applied by means of a follower load on the surface of the inner wall. Moreover, circumferential symmetry conditions were imposed in the lateral areas of the revolution profile .

The finite element mesh used in the simulations was composed of hexahedral elements distributed uniformly in 5 elements for the thickness, 320 elements along the corrugation, and 3 elements in the circular sector, giving a total of $4,848$ elements and $7,816$ nodes considering the cover.

2.3.2 END–TO–END ANASTOMOSIS

Since the selection of the graft is generally made *in–vivo* by means of calipers on the aorta during the surgery, the initial geometry for the finite element model should consider an initial deformation which will also have initial atresses. The present work has considered a Dacron graft of the same diameter of the aorta in diastole (80 mmHg), with a diameter of 24 mm and a thickness of 2 mm (García–Herrera and Celentano, 2013).

Figure 5 schematically shows the boundary conditions for the proposed geometry of the end–to–end anastomosis. It should be noted that between the artery and the Dacron a transition zone has been assumed composed of two materials with slightly better mechanical properties than those of the aorta in order to compensate the discontinuity between the mechanical properties of the aorta and the prosthesis. The above is further supported by the fact that the stitches and teflon bands that help in retaining the graft during the surgery are found in this zone.

In order to understand the influence of the graft under this configuration, it was decided to simulate and evaluate three cases: diastole (80 mmHg), systole (120 mmHg), and hypertension (160 mmHg). Also, to establish comparative relations, the anastomosis was analyzed with segments of young and adult aortas using the parameters of Table 2. In the simulation, a longitudinal stretching $\lambda_z = 1.05$ was included, due mainly to the geometric instability for shorter stretchings, causing errors of numerical convergence.

In the simulation for the Dacron, 280 elements were used in the longitudinal direction and 6 elements for the thickness, and for the aorta 100 elements in the longitudinal direction and 24 elements through the thickness. In both cases a single element was used for the circumferential direction. In the area of the joint the two materials were meshed with greater element density (see Figure 5b). In all, the finite element mesh contains $4,080$ hexahedral elements and $8,790$ nodes.

As mentioned earlier, the geometry for the aorta considered in the anastomosis assumes an initial deformation due to the blood pressure. In this work, an initial geometry has been defined for the diastolic pressure (80 mmHg). Therefore, it is necessary to estimate the stresses associated with this deformation level to describe adequately the response of the material and obviate the high flexibility that there is if they are not taken into account.

The approach to obtain a compatible initial stress field is iteratively tackled by solving the equilibrium equations using the finite element method (García-Herrera et al., 2013; García-Herrera and Celentano, 2013) until the condition of a nearly zero displacement field for the whole aortic is fulfilled (e.g., a maximum admissible diameter variation of 2% was chosen). The numerical simulation of this problem was carried out using the non-linear constitutive model and the corresponding material parameters respectively presented in Section 2.2.

Finally, the stresses are incorporated to the complete model (aorta–Dacron) and, by means of two follower load functions, the Dacron is then pressurized, first at 80 mmHg and afterwards at 120 or 160 mmHg for both the Dacron and the aorta.

3 RESULTS

3.1 PRESSURIZATION TEST

Figure 6 shows the pressure versus circumferential stretch curves for two diferentt λ_z (1.25 and 1.30) values, where the horizontal lines indicate the physiological range between the systole and diastole of the cardiac cycle. Each experimental curve represents the average of a total of 15 cyclic tests. It is seen in Figure 6 that the maximum diametral deformations are low compared to those undergone by the human aorta in the physiological range (García–Herrera et al., 2012).

3.2 ANASTOMOSIS END–TO–END

Figure 7 shows the main maximum stress σ_1 contours in the deformed configuration for the cases mentioned in Section 3.2. The plots incorporate revolution symmetries for their better visualization. The direction of σ_1 nearly coincides with the circumferential direction.

Table 3 shows the principal stresses obtained from the transverse joining plane between the aorta and the Dacron for the two studied cases while Figure 8 shows the failure relation for the anastomotic region defined as $IF_\lambda = \lambda_{max}/\lambda_{rot}$ in the circumferential direction.

4 DISCUSSION

4.1 PRESSURIZATION TEST

The pressurization tests represented in Figure 6 show the high rigidity of the Dacron as it is pressurized from the inside, since the circunferential deformation, both in contraction and elongation, does not exceed 3% after the imposed longitudinal stretching is finished. It is seen that the numerical results represent adequately the biaxial load state. Although the experimental behavior is linear for the pressure range between 80 and 120 mmHg, the numerical results tend to overestimate the response, becoming slightly more rigid for pressures higher than 160 mmHg. The largest differences are seen at the beginning of the simulation and are due mainly to the volumetric change of the matrix, because the fibres in the circumferential orientation are not under load and the diametral stretching λ_θ at low pressure levels affects directly its rgidity. However, for the physiological range of interest the differences are acceptable.

From the inner pressure versus circumferential stretching curves, it is possible to estimate the distensibility (DC) by considering the Dacron as a cylindrical duct based on the outer diameter of the corrugate. This parameter is commonly used to evaluate the in vivo behavior of the blood vessels (Laurent et al., 2005), and it corresponds to the change relative to the vessel span with respect to the arterial pressure:

$$DC = \frac{{D_s}^2 - {D_d}^2}{{D_d}^2(P_s - P_d)} \tag{7}$$

where D_s, D_d, P_s and P_d are different diameters and systolic and diastolic pressures, respectively.

The distensiblity shows 15% differences for a variation of only 5% in λ_z between 1.25 and 1.30. The stretching of the corrugate achieved for $\lambda_z = 1.30$ contributes to ridgidizing the response axially, favouring the dilation of the pressurized segment, with a value of 0.361×10^{-3} mmHg^{-1}.

According to the data published by Tai et al. (2007), for a Dacron graft with a diameter of 5 mm the compliance ($CC = (D_s - D_d/(D_d(P_s - P_d)))$ has a value of 0.19×10^{-3} mmHg^{-1}. Recalculating this parameter for the obtained data, values of 0.158×10^{-3} mmHg^{-1} for $\lambda_z =$ 1.25 and 0.180×10^{-3} mmHg^{-1} for $\lambda_z = 1.30$ are determined. Although these values are in the order of magnitude of the tests, they do not actually indicate the degree of axial stretching undergone by the graft when it is pressurized. However, it is quite similar to that obtained experimentally, with a lower difference of 5.6% for $\lambda_z = 1.30$. In the present work, it has been assumed as a reasonable approximation that the functional stretching will correspond to $\lambda_z = 1.30$, mainly because with this value the buckling caused by the pressurization disappears at pressures lower than 200 mmHg, although it could be overestimated due to the anchoring conditions undergone by the prosthesis when it is inserted in the body.

Qualitatively, both for the experiments and simulation, at $\lambda_z = 1.30$ and a pressure close to 240 mmHg, the material still does not succeed in reducing the waves in the corrugate. Furthermore, no effect can be seen on the fixing of the sample with the cover, because the distribution of the radial displacements on the profile is uniform after the second wave from the cover. This generates a stress field with an axially periodic distribution due to the freedom offered by the unstretched corrugate once the longitudinal stretching prior to the pressurization is finished. More specifically, from the numerical results it is seen that maximum concentrations stand out towards the inner radii of the corrugated profile, with stress values of 3.46 MPa for $\lambda_z = 1.25$ and 4.24 MPa for $\lambda_z = 1.30$ for the circumferential stress, approximately one order of magnitude greater than the stresses in the outer radii. In the case of the longitudinal stresses, values of 0.985 MPa fo $\lambda_z = 1.25$ and 1.47 MPa for $\lambda_z = 1.30$ at the inner edges are obtained.

In the pressurization problem analyzed, one end of the domain is closed and, in addition, the filling flow rate is low. Therefore, the problem is well represented by a quasistatic model in which the fluid only exerts pressure on the internal wall. The extension of this study to pulsatile flows, where an output valve should be considered to experimentally adjust the pressure, the simulation should also include the viscous effects of the fluid and the interaction with the Dacron wall

4.2 ANASTOMOSIS END–TO–END

With respect to the proposed case of the end-to-end anastomosis, a simple way to evaluate the performance for this configuration is to determine the value of the distensibility DC at points of interest, e.g., at the joint between the Dacron and the aorta and in zones away from it for each material. Also, as an additional comparison, the pressurization for an aortic segment under identical surrounding conditions for the cases of a healthy young and an aged aorta at $\lambda_z = 1.05$ (control cases) has been simulated.

As to the aortic segments distant from the anastomosis, it was determined that the insertion of the prosthesis decreases the distensibility around 3.2% and 8.6% with respect to the control cases of young and aged aorta, respectively, in view of the axial flexibility induced by the graft, and considering that to calculate the control cases an isotropic model was used, with values of 4.291×10^{-3} mmHg^{-1} for the young case and 9.635×10^{-3} mmHg^{-1} for the aged case. However, if these cases are compared with those of the Dacron and and the joint between both tissues, the changes induced in the vessel will modify completely the stress and deformation levels. In the case of the joint, the distensibility difference gets to be five times smaller, denoting an important loss of elasticity for dilation in the case of the healthy young vessel, and getting about seven times more rigid in the case of an adult aorta at a stretching $\lambda_z = 1.05$. This phenomenon was also predicted by Chandran et al., 1992 using a linear elastic model.

On the other hand, the distensibility values for Dacron decrease by about 50% in the case of a young aorta and 33% of the adult with respect to the experimental stretching values at $\lambda_z = 1.30$. The above implies that the replacement tissue under these configurations undergoes a considerable alteration of the aorta's elastic capacity, decreasing approximately 25 times in the young case and 44 times in the adult. These differences can eventually cuse adverse effects in the behavior of the blood flow, because this decrease will affect one of the main functions of the ascending aorta, which is the damping of the pressure wave from the left ventricle of the heart.

The proposed geometry corresponds to a particular case associated with the end of the replacement surgery, because due to the cardiovascular cycle the graft will tend to dilate because of the rate-dependent effect of the material and to increase the longitudinal stretching to a state of equilibrium (Etz et al., 2007; Zilla et al., 2007). It must also be considered that the mechanical response of the aorta considers a model that does not take into account the reorientation of the collagen fibres, and therefore it does not captare its own rigidization in the circumferential direction and overestimates its performance (García-Herrera et al., 2012). Now, considering that for a stable state the graft achieves a longitudinal stretching close to $\lambda_z = 1.30$, se observaran rigidity differences 12 and 26 times more rigid are seen for young and adult patients, respectively.

Comparing in Figure 7 the stress states between 120 and 160 mmHg, the differences between the mechanical properties for the young and adults aortas are seen, finding a greater requirement in the neighborhood of the anastomatic zone towards the Dacron segment with a maximum stress σ_1 of 1.43 MPa and 2.38 MPa, for the cases of hypertensive young and adult aortas, respectively, as a consequence of the early rigidizing response of adult tissues. However, the stresses generated within the physiological range involve a similar behavior between both materials for the deformations as well as for the maximum stresses, leading to similar stresses for the Dacron graft with a value of 0.98 MPa in systole.

The stresses generated in the anastomotic plane summarized in Table 3 show that the stress gradient in the neighborhood of the anastomosis suffers a drastic change, concentrating all the stress in the change of section between both materials due to the different diameters, causing greater circumferential stresses on the Dacron segment. In relation to the stresses in the initial configuration (80 mmHg), as a result of the stretching of the graft important stresses appear in the longitudinal direction (σ_2) of the same order as the main stress, and it is 25% smaller than it. As the pressure increases, the difference between the main stresses varies considerably for σ_1, reaching crtical values in the case of an adult aorta, with 1.28 MPa in hypertension. Now, comparing these values with the breakage stress in the circumferential direction (see Table 2), a failure relation ($IF_\sigma = \sigma_{max}/\sigma_{rot}$) around 0.30 is obtained for the healthy young aorta, and close to one for the adult under a hypertension condition.

Another way of evaluating the danger in the anastomotic region is by determining the ratio of the maximum main stretching to the breakage stretching. Figure 8 shows a high deformation concentration in the inner zone of the joint. Few differences are seen in this parameter as the pressure is increased, taking values of 0.52 for the young aorta case, and 0.65 for the adult aorta in systole. It is seen that the stretching levels are far from the rupture, however under contour conditions that involve the displacement and rotation that the graft inserted next to the aortic root will undergo (García-Herrera and Celentano, 2013), these values increase, and this zone (anastomosis) is potentially prone to the tearing of the inner wall of the vessel, especially in patients of advanced age. This shows the complex situation to which the aorta is subjected after replacing the damaged tissue, where possibly because of these stresses pseudoaneurysms or dissections may appear in the aortic wall. However, for an adequate representation of the end–to–end anastomosis the effects of the stitching and the surgical adhesive which contribute structurally to the reception process of the graft should also be considered.

It must be stressed that the simulations do not consider the effect of the remodeling (adaptation and growth) of the vascular wall, because the concentration of stresses in the anastomosis zone will generate important consequences due to the neointimal hyperplasia in this region, increasing the shear stresses caused by the blood flow, and changing the geometry as a consequence of the rigidization of the arterial wall (Zilla et al., 2007). Yet the validity of the simulation provides information under static hypotheses after the insertion of the graft, where rate-dependent effects due to the arterial pressure as well as to the remodeling have little significance. It should also be mentioned that the use of an isotropic model in the simulations will overestimate the stresses at low stretching levels, and therefore by using an anisotropic model the stresses will represent directly the response depending on the directions of the fibres present in the arterial wall, and in this way the levels of demand will be smoothed in the anastomosis.

Moreover, to study the displacement evolution of the end-to-end anastomosis in presence of pulsatile flows, it should be necessary, once again, to include in the simulations the effects of the fluid viscous stresses on the internal walls both the artery and graft.

5 CONCLUSIONS

Experimental data of pressurization tests set up in vitro and numerical results have been presented, in this way validating an anisotropic constitutive model capable of predicting the mechanical response of a woven Dacron graft. Then the performance of the end-to-end anastomosis between the Dacron and the aorta, simulating the post-operative situation, has been analyzed with the purpose of determining the result of the stress condition of the insertion of the prosthesis in cases of a healthy young and adult aorta. In both cases an important loss of elasticity occurs, manifested by the decrease of the distensibility of the anastomotic region, as well as a significant difference with respect to the replacement tissue. As to the generated stresses, there are high concentrations at the inner joining of the two tissues, which becomes a potential zone for tearing that increases in older patients. The differences between the mechanical properties will affect the normal functioning of the cardiovascular cycle and in particular the lack of distensibility will affect the damping of the pressure wave. The limitations of this work must be dealt with in future research, considering assumptions in the constitutive modeling (for example, incorporating the rate-dependent response and the interaction between fibres), and complementing the study for cases that involve the response of the aortic arch under conditions of the surroundings equivalent to the physiological load.

6 CONFLICTS OF INTEREST

The authors have no conflicting interests regarding this paper.

7 ACKNOWLEDGEMENTS

The supports provided by the DICYT Project No. 051415GH of the Universidad de Santiago de Chile (USACH) and the FONDECYT Project No. 1151119 of the Chilean Council for Research and Technology (CONICYT) are gratefully acknowledged.

8 REFERENCES

Beller, C. J., Labrosse, M. R., Thubrikar, M. J. and Robicsek, F., 2004. Role of aortic root motion in the pothogenesis of aortic dissection. Circulation 109, 763-769.

Berger, K. and Sauvage, L. R., 1981. Late fiber deterioration in dacron arterial grafts. Ann Surg 193(4), 477-491.

Bustos, C. A., García–Herrera C. M. and Celentano, D. J., 2015. Mechanical characterisation of Dacron graft: Experiments and numerical simulation. Journal of Biomechanics, (in Press) 2015.

Chandran, K. B., Gao, D., Han, G., Baraniewski, H., and Corson, J. D., 1992. Finite-element analysis of arterial anastomoses with vein, Dacron and PTFE grafts. Medical & Biological Engineering & Computing, 30, 413-418.

De Paulis, R., Scaffa, R., Maselli, D., Salica, A., Bellisario, A. and Welter, L., 2008. A third generation of ascending aorta dacron graft: Preliminary experience. Ann Thorac Surg 85, 305-309.

Doty, D. B. and Doty, J. R., 2012. Cardiac Surgery: Operative technique. Elsevier.

Etz, C. D., Homann, T., Silovitz, D., Bodian, C. A., Luhuer, M., Di Luozzo, G., Konstadinos, A. P. and Griepp, R. B., 2007. Vascular graft replacement of the ascending and descending aorta: Do dacron grafts grow?. Ann Thorac Surg 84, 1206-1213.

García–Herrera, C. M., Celentano, D. J., Cruchaga, M. A., Rojo, F. J., Atienza, J. M., Guinea, G. V. and Goicolea, J. M. 2012. Mechanical characterisation of the human thoracic descending aorta: experiments and modelling. Computer Methods in Biomechanics and Biomedical Engineering 15, 185-193.

García–Herrera, C. M. and Celentano, D. J., 2013. Modelling and numerical simulation of the human aortic arch under in vivo conditions. Biomech Model Mechanobiol 12, 1143-1154.

García–Herrera, C. M., Celentano, D. J. and Cruchaga, M. A. 2013. Bending and pressurization test of the human aortic arch: Experiment, modelling and simulation of patient-specific case. Computer Methods in Biomechanics and Biomedical Engineering 16(8), 830-839-193.

Guinea, G. V., Atienza, J. M., Elices, M., Argoncillo, P. and Hayashi, K. 2005. Thermomechanical behavior of human carotid arteries in the passive state. AJP – Heart Circ Physiol 115, 481-488.

Hasegawa, M. and Azuma, T., 1979. Mechanical properties of synthetic arterial grafts. J Biomechanis 12, 509-517.

Holzapfel, G. A., 2000. Non linear solid mechanics. John Wiley & Sons Ltd., Chichester.

Lee, J. M. and Wilson, G. J., 1986. Anisotropic tensile viscoelastic properties of vascular graft material tested at low strain rates. Biomaterials 7, 423-431.

Martínez–Hernández, H., 2006. Los aneurismas de la aorta torácica y su enfoque terapéutico. Archivos de cardiología de México 76(2), 124-133.

Planas, J., Guinea, G. V. and Elices, M., 2007. Constitutive model for fiber-reinforced materials with deformable matrices. Physical Review E 76(4), 1539-3755.

Ramírez, A., Careaga, C., Teéllez, S. and Arguero, R., 2003. Tratamiento quirúrgico de los aneurismas de la aorta torácica. Revista Mexicana de Cardiología 14(4), 118-127.,

Tai, N. R., Salacinski, H. J., Edwards, A., Hamilton, G. and Seifalian, A. M. 2007. Compliance properties of conduits used in vascular reconstruction. British Journal of Surgery 87, 1516-1524.

Tremblay, D., Zigrasa, T., Cartier, R., Leduc, L., Butany, J., Mongrain, R. and Leask, R. L., 2009. A comparison of mechanical properties of materials used in aortic arch reconstruction. Ann Thorac Surg 88, 1484-1491.

Van Damme, H., Deprez, M., Creemers, E. and Limet, R., 2005. Intrisic structural failure of polyester (Dacron) vascular grafts: A general review. Acta chir belg 105(3), 249-255.

Vardoulis, O., Coppens, E., Martin, B., Reymon, P., Tozzi, P. and Stergiopulos, N., 2011. Impact of aortic grafts on arterial pressure: A computational fluid dynamics study. Eur J Vasc Endovasc Surg 42, 704-710.

Zilla, P., Bezuidenhout, D. and Human, P., 2007. Prosthetic vascular grafts: Wrong model, wrong questions and no healing. Biomaterials 28, 5009-5027.

Figure 1: Analyzed Dacron prosthesis (Bustos et al., 2015).

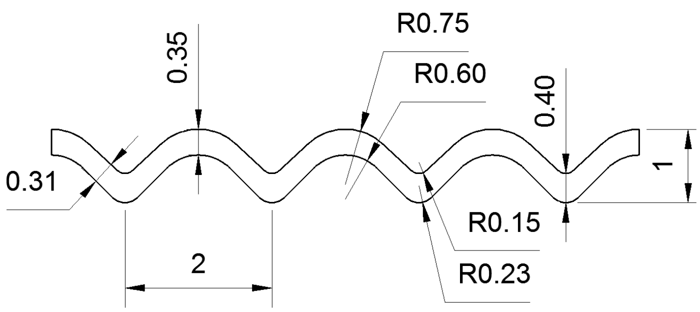

Figure 2: Detail of the corrugation of the tested Dacron prosthesis. Sizes in millimeters (Bustos et al., 2015).

Figure 3: Setup of the pressurization test in the testing machine. On the left, attachment of the sample to the nozzles, and on the right, setup of the extensometer and axial stretching.

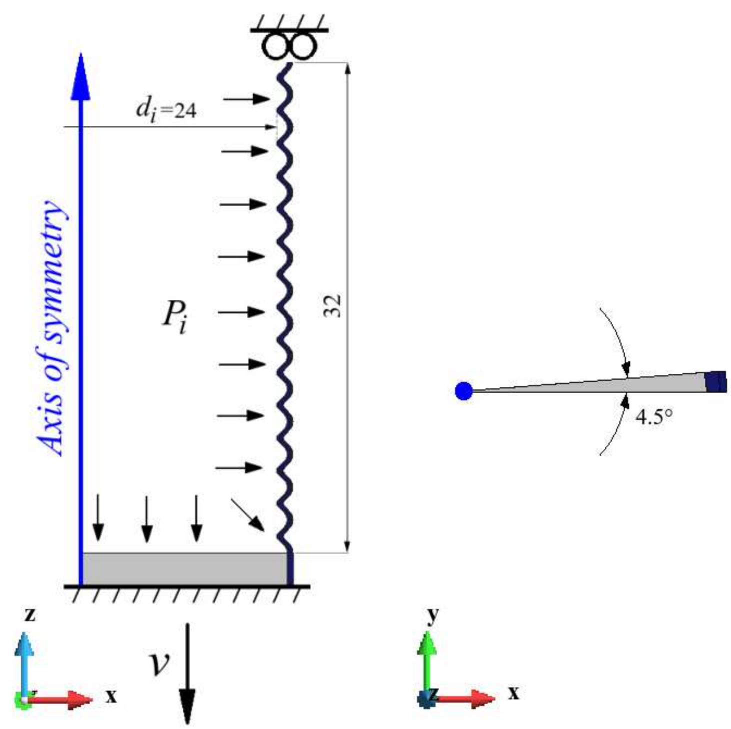

Figure 4: Schematic of the boundary conditions in relation to the revolution profile in the XZ and XY planes (dimensions in mm).

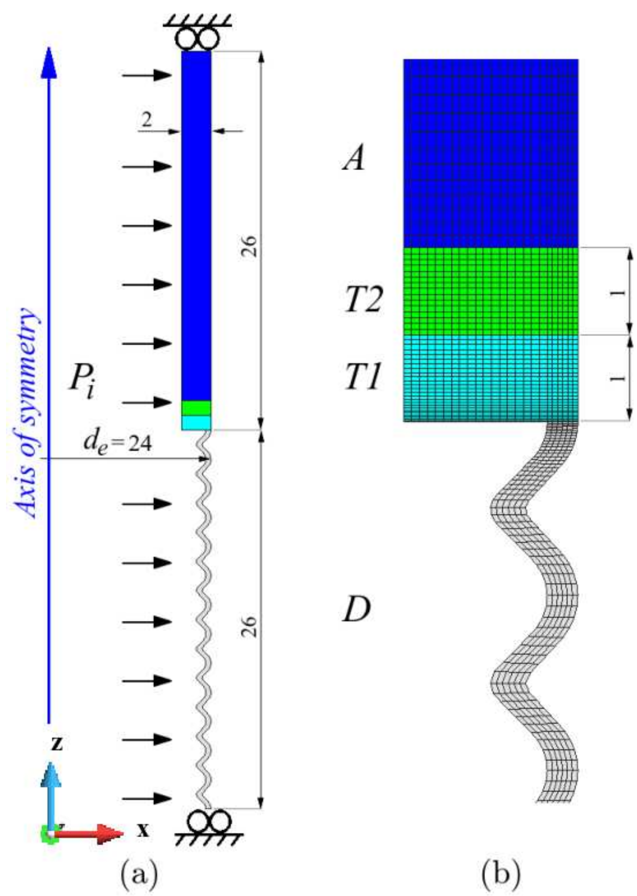

Figure 5: (a) Geometry considered for the end–to–end anastomosis. (b) Detail of the mesh at the joint of the two materials, where A: healthy aorta; T1: transition 1; T2: transition 2; and D: Dacron (dimensions in mm).

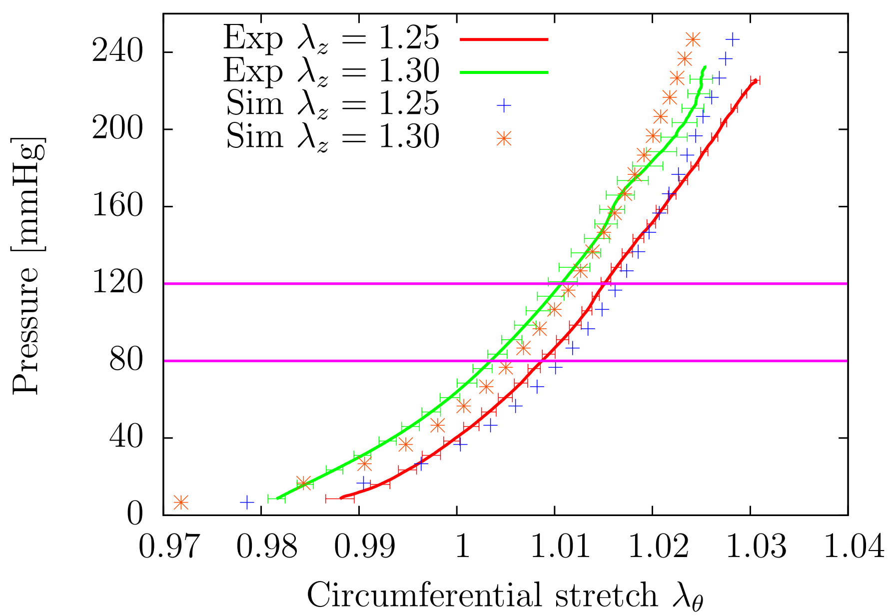

Figure 6: Experimental measurements and numerical results of pressure versus circumferential stretch for $\lambda_z = 1.25$ and $\lambda_z = 1.30$.

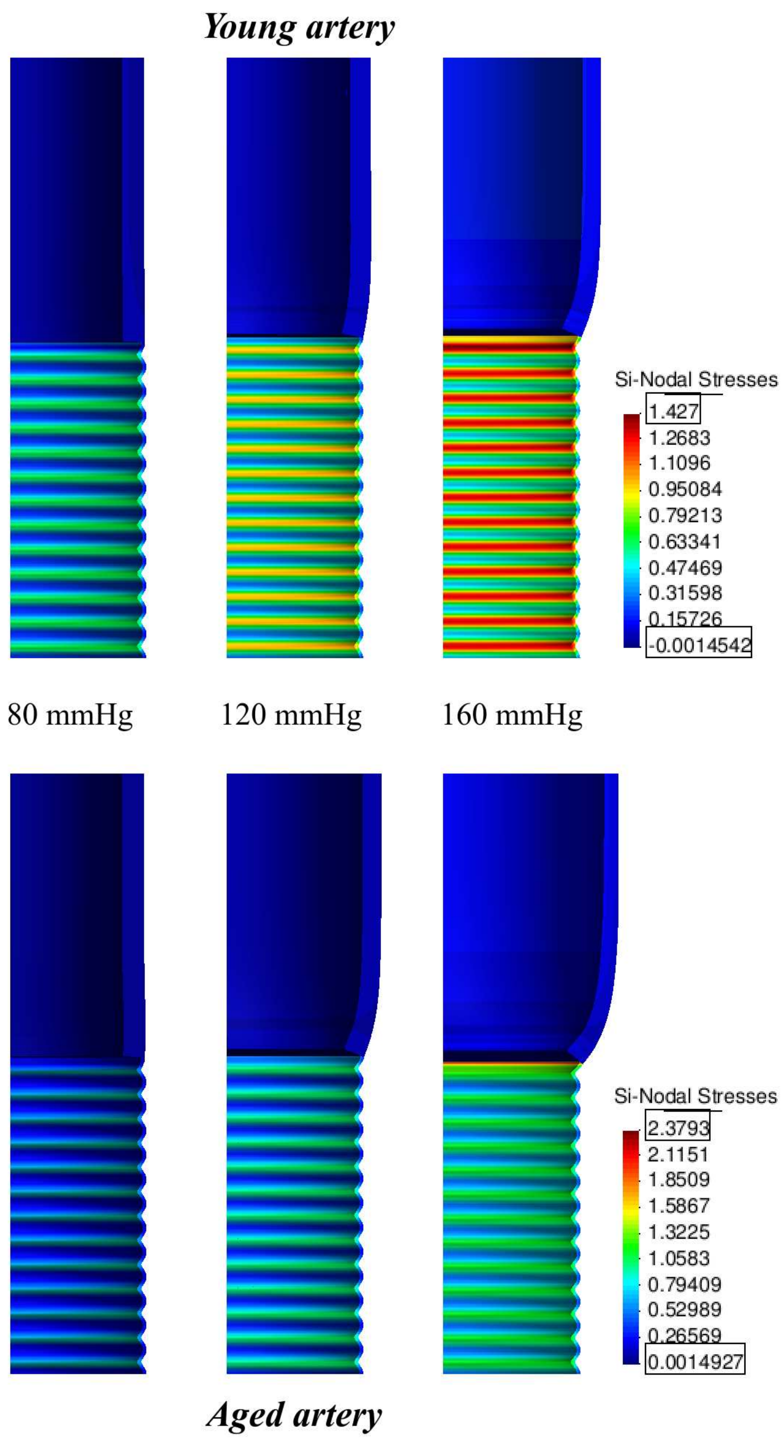

Figure 7: Stresses σ_1 [MPa] of the deformed configuration for the normotensive and hypertensive conditions at $\lambda_z = 1.05$ of the cases with healthy young and adult aortas.

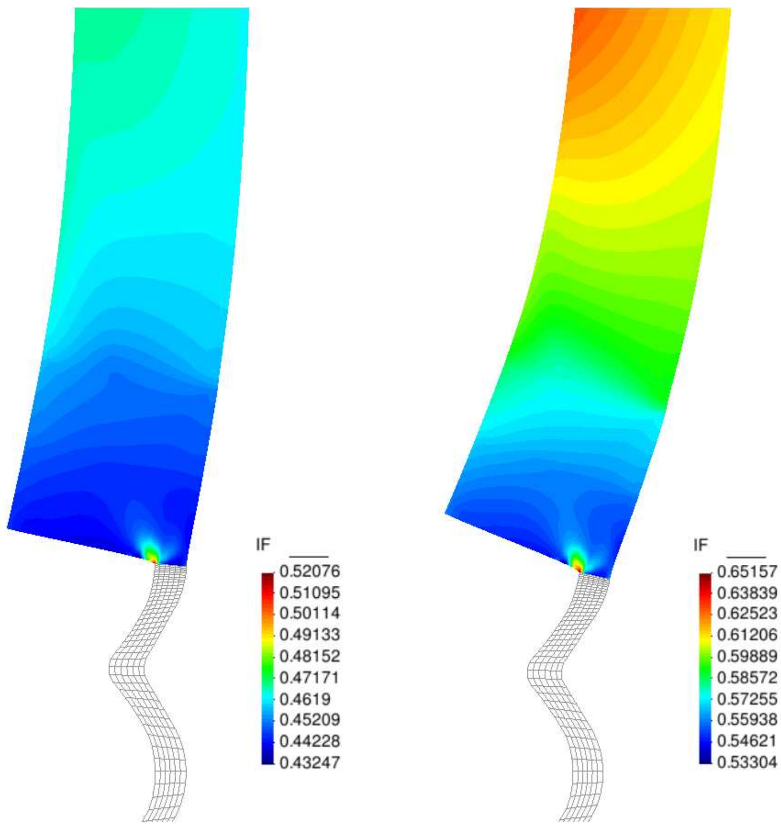

(a)

(b)

Figure 8: Failure index IF_λ in the profile of the anastomatic region of the cases with a healthy (a) young and (b) adult aorta in systole (120 mmHg).

μ [kPa]	K_1 [kPa]	K_2 [kPa]	K_3 [kPa]	${f_f}^{circ}$	${f_f}^{long}$
60.596	10.234	1.852×10^{-3}	14.20×10^6	0.95	0.05

Table 1: Material parameters for the Dacron graft (Bustos et al., 2015).

Age	a [kPa]	b	$\lambda_{rot} \pm EE_\lambda$	$\sigma_{rot} \pm EE_\sigma$ [MPa]
Young (16–36)	$104,004$	$0,844$	2.34 ± 0.05	2.281 ± 0.236
Aged (38–62)	$54,419$	$1,936$	1.90 ± 0.05	1.284 ± 0.349

Table 2: Material parameters and circumferential rupture limits for the segments of ascending aorta (García–Herrera and Celentano, 2013).

Pressure		80 mmHg	120 mmHg	160 mmHg
Young artery	σ_1 [kPa]	195.25	286.35	687.17
	σ_2 [kPa]	156.07	259.74	335.02
Aged artery	σ_1 [kPa]	198.73	410.27	1286.40
	σ_2 [kPa]	157.04	273.14	330.31

Table 3: Principal stresses σ_1 and σ_2 obtained in the anastomosis plane under normotensive and hypertensive loads.